



CHORUS

This is the accepted manuscript made available via CHORUS. The article has been published as:

Superelastic rescattering in single ionization of helium in strong laser fields

Zhi-Chao Li, Agnieszka Jaron-Becker, and Feng He

Phys. Rev. A **94**, 043406 — Published 5 October 2016

DOI: [10.1103/PhysRevA.94.043406](https://doi.org/10.1103/PhysRevA.94.043406)

Superelastic Rescattering in Single Ionization of Helium in Strong Laser Fields

Zhi-Chao Li^{1,2}, Agnieszka Jaron-Becker² and Feng He^{1,3*}

¹ *Key Laboratory for Laser Plasmas (Ministry of Education) and Department of Physics and Astronomy, Shanghai Jiao Tong University, Shanghai 200240, People's Republic of China*

² *JILA and Department of Physics, University of Colorado, Boulder, Colorado 80309-0440, USA*

³ *Collaborative Innovation Center of IFSA (CICIFSA), Shanghai Jiao Tong University, Shanghai 200240, China*

Rescattering is a central process in ultrafast physics, in which an electron, freed from an atom and accelerated by a laser field, loses its energy by producing high-order harmonics or multiple ionization. Here, taking helium as a prototypical atom, we numerically demonstrate superelastic rescattering in single ionization of an atom. In this scenario, the absorption of a high-energy extreme ultraviolet (EUV) photon leads to emission of one electron and excitation of the second one into its first excited state, forming He^{+*} . A time-delayed mid-infrared laser pulse accelerates the freed electron, drives it back to the He^{+*} and induces the transition of the bound electron to the ground state of the ion. Identification of the superelastic rescattering process in the photoelectron momentum spectra provides a means to determine the photoelectron momentum at the time of rescattering without using any information of the time-delayed probe laser pulse.

PACS numbers: 42.65.Ky, 32.80.Rm, 32.30.Jc, 34.80.Qb

I. INTRODUCTION

The advent of ultrashort laser technologies has driven studies of ultrafast laser physics [1]. A series of intriguing ultrafast scenarios of atoms and molecules in strong laser fields have been explored in past years [2–5], among which rescattering is a key, or even the most important process [6, 7]. For an atom or molecule exposed to an external laser field, the valence electron may tunnel out the laser-distorted Coulomb potential [8], followed by the electron acceleration in the laser field. When the laser field changes its direction, the freed electron is driven back and rescatters with its parent core [9]. During the rescattering, the freed electron may release its kinetic energy as high-order harmonics upon recombination with the parent ion [9, 10], which can be synthesized into attosecond pulses providing time rulers with unprecedented time resolutions [11]. Alternatively, the rescattering electron may share its energy with other electrons in the parent ion. Depending on the energy that the electron transfers, a second electron may be directly knocked out, resulting in nonsequential double ionization [7, 12–14], or be pumped to some excited states which will be subsequently tunneling ionized by the field [15, 16]. Recently, Deng *et al.* further demonstrated inner-shell excitation by rescattering followed by x-ray emission [17]. In molecules, the rescattering electron may excite the parent molecular ion to repulsive states, thus initiating molecular dissociation or Coulomb explosion [18–21]. The corresponding signals, either photoelectron momentum yields, or high-order harmonics spectra, or dissociative fragments kinetic energy spectra, carry information about the target as well as the laser field. For example, the

rescattered high-energy photoelectrons from N_2 and O_2 are shown to contain information about the time-resolved molecular bond stretching with superhigh spatial resolutions [22], or high-order harmonic yields or rescattering photoelectron energy spectra can be used to calibrate the carrier envelope phase of a few-cycle infrared laser pulse [23, 24]. All these processes have in common, that the freed electron loses all or part of its kinetic energy during the rescattering process. Thus, we refer to these scenarios as inelastic rescattering in order to distinguish from the superelastic rescattering, which we will present and discuss in the present letter.

Choosing the helium atom as a prototypical target, we conceive a numerical experiment to demonstrate superelastic rescattering in single ionization of helium in strong laser fields. In this process, an EUV pulse is used to free one electron from the helium atom, while the other electron is excited to one of the excited states forming a He^{+*} ion. The freed electron is then driven back by a time-delayed mid-infrared (MIR) pulse to rescatter with the parent ion. Instead of sharing its energy with the bound electron or completely transforming its kinetic energy into the energy of a high harmonic photon, the freed electron extracts the energy stored in the He^{+*} ion by de-exciting the bound electron in the He^{+*} into its ground state. This process is termed as superelastic rescattering. As we will show below, the process can be identified in photoelectron momentum spectra, which allows us to extract details of electron-electron correlation.

II. NUMERICAL MODEL

The numerical solution of the time-dependent Schrödinger equation (TDSE) for a helium atom in EUV fields by including two electrons with full dimensions has been carried out for exploring many interesting phenom-

* fhe@sjtu.edu.cn

ena [25–30]. However, simulating two-electron dynamics in full dimensions in long-wavelength laser fields is still a tremendous computational task. Furthermore, a two-electron model in reduced dimensions has often been used to qualitatively identify physical scenarios, such as non-sequential double ionization [31], or the role of Fano resonances [32, 33]. While such a one-dimensional model overestimates the effect of electron-electron correlation, it is known to provide qualitative insights into the relevant physical processes. Thus, we simulate the TDSE for the helium atom in the combined EUV and mid-infrared field by confining the electron movement along the laser polarization axis (atomic units, $e = m = \hbar = 1$, are used unless indicated otherwise):

$$i\frac{\partial}{\partial t}\Psi(x_1, x_2; t) = \left[\frac{[p_1 + A(t)]^2}{2} + \frac{[p_2 + A(t)]^2}{2} + V(x_1, x_2) \right] \Psi(x_1, x_2; t), \quad (1)$$

where the Coulomb potential is modeled as

$$V(x_1, x_2) = -\frac{2}{\sqrt{x_1^2 + s_1}} - \frac{2}{\sqrt{x_2^2 + s_1}} + \frac{1}{\sqrt{(x_1 - x_2)^2 + s_2}}. \quad (2)$$

In Eq. (1), p_1 and p_2 are the momentum operators of two electrons e_1 and e_2 , $A(t)$ is the laser vector potential with $A(t) = -\int_{-\infty}^t E(t')dt'$ where $E(t)$ is the combined electric field of the two laser pulses. The two soft-core parameters are $s_1 = 0.5$ and $s_2 = 0.339$, such that the ground state energy of the He atom model is -2.9 a.u., and the ground state energy of He^+ is -2.0 a.u.. The imaginary time propagation method was used to calculate energy levels and eigenstates. We sampled the simulation grid with 25000×25000 points of equidistant spacing $\Delta x_1 = \Delta x_2 = 0.2$ a.u.; the time step was $\Delta t = 0.1$ a.u.. To suppress the unphysical reflection from boundaries, a mask function of $\cos^{1/6}$ was applied [34]. Convergence of the results with respect to the grid parameters has been tested.

The combined EUV and MIR field is given by $E(t) = E_E(t) + E_M(t)$, where

$$E_E(t) = E_{E0} \sin[\omega_E(t + \Delta t)] \cos^2 \left[\frac{\pi(t + \Delta t)}{\tau_E} \right], \quad (3)$$

$$-\frac{\tau_E}{2} - \Delta t < t < \frac{\tau_E}{2} - \Delta t$$

$$E_M(t) = E_{M0} \sin(\omega_M t) \cos^2 \left(\frac{\pi t}{\tau_M} \right), \quad -\frac{\tau_M}{2} < t < \frac{\tau_M}{2} \quad (4)$$

The amplitudes are $E_{i0} = \sqrt{\frac{I_i}{3.51 \times 10^{16}}}$ and $E_i(t)$ equals zero outside the specified time intervals, where i indicates the EUV or the MIR field. To distinctly see the superelastic rescattering processes, we set $I_E = 10^{16}$ W/cm² in order to generate He^{+*} with large probabilities. The EUV frequency is varied around 2.2 a.u.. The MIR wavelength has been chosen to be equal to 1600 nm, and its intensity as 2×10^{14} W/cm². We have chosen the wavelength and intensity such as to avoid MIR-induced ionization of He^{+*} , but supplying a strong electric force to

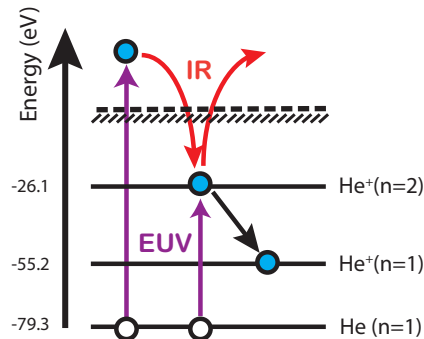


FIG. 1. (color online) Schematic energy-level diagram of the model He atom. The EUV pulse simultaneously ionizes one electron and excites the other one, producing He^+ in the $n = 2$ state. The time-delayed MIR pulse drives the free electron back to He^+ ($n=2$) and extracts the energy stored in He^+ ($n = 2$) by deexciting the second electron to the ground state of the ion.

drive the EUV-freed electron back to its parent ion core. $\tau_E = 40$ and $\tau_M = 1.5$, scaled in cycles of the corresponding fields. By restricting the MIR field less than two cycles, we avoid more than two rescattering events which makes the identification and analysis of the process easier.

The mechanism related to superelastic rescattering is sketched via the energy level diagram in Fig. 1. By absorbing one EUV photon, a free electron and He^{+*} ($n = 2$, where n is the principle quantum number) are produced simultaneously. The freed electron propagates out with the initial velocity $\pm\sqrt{2(\omega_E - I_p - \Delta E_{21})}$, where I_p is the single ionization potential of He and ΔE_{21} is the energy difference between the ground and first excited state of He^+ . In this model, $I_p = 0.9$ a.u., $\Delta E_{21} = 1.1$ a.u.. Subsequently, the MIR field drives the freed electron back to the parent He^{+*} ion. During rescattering, different from all previous reported processes [7], the freed electron extracts the energy ΔE_{21} stored in He^{+*} by deexciting the second electron back to the ground state instead of sharing its energy with the bound electron. Consequently, besides overcoming the single-ionization potential, all the excess EUV photon energy is finally deposited in the freed electron.

III. SIMULATION RESULTS

In order to identify the superelastic rescattering process, we first look at the ionization of He when only the EUV pulse is introduced. Fig. 2 (a) shows the electron wave function in the space representation after the interaction of the EUV pulse. In the four quadrants where $|x_1| > 10$ and $|x_2| > 10$, the double ionization events triggered by simultaneously absorbing two EUV photons emerge. The single ionization events are defined as the wave packets distributed in the areas $|x_1| < 10$

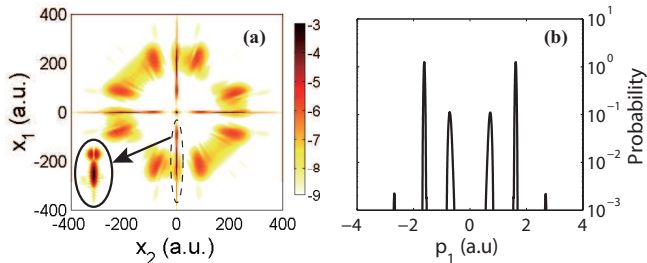


FIG. 2. (color online) (a) The wave function distribution in a logarithmic scale after the EUV pulse is terminated. (b) The photoelectron momentum spectrum associated with the single ionization of helium atom. The inset in (a) is the zoom of the single ionization region marked by the ellipse. The EUV intensity and frequency was 10^{16} W/cm² and $\omega_E = 2.2$ a.u..

and $|x_2| > 10$, or $|x_2| < 10$ and $|x_1| > 10$. A zoom of the single ionization region marked by the dashed oval is shown in the inset, in which two distinct parts without and with nodes at $x_2 = 0$ correspond to He⁺ in the states of $n = 1$ and $n = 2$, respectively. By performing the Fourier transformation for the singly ionized wave function $\Psi_{\text{ion}}(x_1, x_2; t_f)$ at the terminal time t_f , we obtained the single ionized wave function in momentum representation

$$\tilde{\Psi}(p_1, p_2) = \frac{1}{2\pi} \int \int \Psi_{\text{ion}}(x_1, x_2; t_f) e^{-i(p_1 x_1 + p_2 x_2)} dx_1 dx_2. \quad (5)$$

Note that p_1 and p_2 here are canonical momenta. The photoelectron momentum distribution of single ionization is $W(p_1) = \int |\tilde{\Psi}(p_1, p_2)|^2 dp_2$, as shown in Fig. 2 (b), where the two highest and two inner peaks, named as fast and slow electrons for convenience, are associated with He⁺ in $n = 1$ and $n = 2$ states, respectively. The two tiny peaks at $p_1 = \pm 2.65$ a.u. are correspond to two-EUV-photon single ionization, which will not be considered further below, since rescattering with He⁺ cannot be induced by the time-delayed MIR pulse introduced in the following.

When the MIR field is introduced at a proper time delay, electrons with the lower energy may be steered back to its parent ion core. Fig. 3 (a) shows the combined EUV and MIR field at a time delay $\Delta t = 220$ a.u. (i.e., one full MIR cycle). Assuming that the electron is liberated at the center of the EUV pulse with the initial momentum -0.7 a.u., the red dashed curve in Fig. 3 describes the electron trajectory by solving the Newton equation without including the Coulomb potential. The electron may rescatter with its parent core at $t_{r1} = -5$ a.u. or $t_{r2} = 265$ a.u.. For the MIR parameters we used here, the electrons emitted with momenta (peaked at $+0.7$ a.u. and ± 1.7 a.u. in Fig. 2(b)) will not be driven back to the parent ion. Fig. 3 (b) presents the snapshot of the electron distribution at $t = 110$ a.u. (i.e. half a MIR cycle), while the corresponding singly-ionized photoelec-

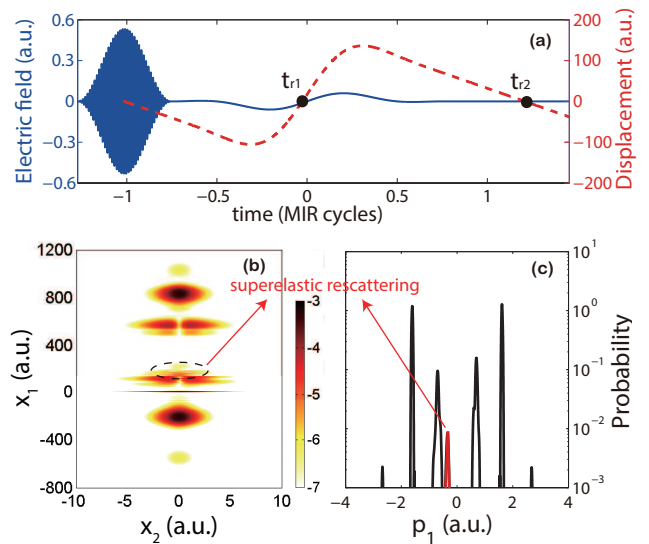


FIG. 3. (color online) (a) The superimposed EUV and MIR fields (blue solid curve) and a typical electron trajectory (red dashed curve). t_{r1} and t_{r2} represent two rescattering instants obtained by solving the Newton equation without including the Coulomb potential. (b) The wave function distribution at $t = 110$ a.u. (half a MIR cycle). (c) The canonical momentum spectrum for the single ionization at $t = 110$ a.u.. The time delay between the EUV and MIR pulses is 220 a.u. (one full MIR cycle).

tron momentum spectrum is shown in Fig. 3 (c). The full propagation of the wave function can be found in the movie in the supplementary material [35].

By watching the wave function propagation, one can identify that the slow electron propagating along $-x_1$ emitted due to the interaction with the EUV pulse reverses its motion in the MIR field and rescatters with the He⁺, as expected. After the rescattering wave packet passes the region of $x_1 = 0$, the node of the wave packet at $x_2 = 0$ is partly filled (as shown by the dashed oval in Fig. 3(b)), indicating the deexcitation of the bound electron e_2 from the $n = 2$ to $n = 1$ state. Compared to Fig. 2 (b), in the photoelectron momentum spectrum a new peak in Fig. 3 (c) appears at $p_1 = -0.34$ a.u. (red solid line), which exactly corresponds to the energy given by the superelastic rescattering scenario. Note that the kinetic momentum at t_{r1} can be obtained by shifting the canonical momentum by $A(t_{r1})$. Consequently, the new (red) peak shows up at a larger kinetic momentum, illustrating the electron acceleration during the superelastic rescattering process. We parenthetically point out that the freed electron might miss the He⁺ ion in the first rescattering, but deexcite He⁺ in the second reencounter at about t_{r2} , which is not further analyzed here.

The contribution to the photoelectron momentum spectrum due to the superelastic rescattering processes offers a perspective to visualize details about the rescattering process itself. For example, the rescattering time and the momentum of the rescattered electron can be es-

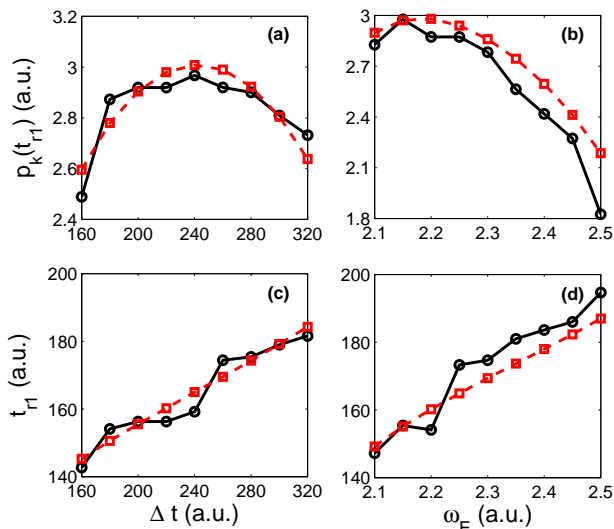


FIG. 4. (color online) The rescattering momentum $p_k(t_{r1})$ (up row) and rescattering timing t_{r1} (lower row) as a function of the time delay at $\omega_E = 2.2$ a.u. (left column) and the EUV frequency at $\Delta t = 220$ a.u. (right column). The red dashed and black solid curves are obtained from classical calculations and the TDSE simulations, respectively.

timated as follows. During the superelastic rescattering process, the energy stored in He^{+*} ($n = 2$) is transferred to the free electron, i.e.,

$$\Delta E_{21} = \frac{[p_k(t_{r1}) + \Delta p]^2}{2} - \frac{p_k^2(t_{r1})}{2}, \quad (6)$$

where $p_k(t_{r1})$ is the photoelectron kinetic momentum at the moment of rescattering and Δp is the momentum increment during superelastic rescattering. Since both the momenta of the slow electron and the new momentum peak (occurring due to superelastic rescattering, i.e. the red peak in Fig. 3 (c)) are both streaked by the MIR field simultaneously, Δp remains unchanged if the Coulomb effect on the freed electron is assumed to be negligible. From Eq. (6) we derive the electron kinetic momentum at the instant of rescattering as

$$p_k(t_{r1}) = \Delta E_{21}/\Delta p - \Delta p/2. \quad (7)$$

The black solid lines in Figs. 4 (a) and (b) show the results of our TDSE simulations for the dependence of $p_k(t_{r1})$ on the time delay and EUV frequency, respectively. One may further derive the superelastic rescattering instant t_{r1} from $A(t_{r1})$ by using $A(t_{r1}) = p_k(t_{r1}) - p_i$, providing that $A(t)$ is known, with $p_i = -\sqrt{2(\omega_{EUV} - I_p - \Delta E_{21})}$ and assuming that the Coulomb potential can be neglected. The predictions for the rescattering instants t_{r1} as a function of the time delay and ω_{EUV} , based on our TDSE simulations, are shown in Figs. 4 (c) and (d) by the black

solid curves, respectively. The trends in Figs. 4 (c) and (d) clearly demonstrate that for a larger time delay or EUV frequency, the freed electron will propagate further out, and it requires a longer time to drive the electron back to the parent ion by the MIR field. As reference, in Fig. 4 we also present the corresponding classical predictions obtained by solving the Newton equation without including the Coulomb potential $\frac{dp_k(t)}{dt} = -E_M(t)$ with the initial momentum and displacement being p_i and 0, respectively. In these classical calculations, the rescattering momenta and time are extracted by tracing the electron trajectories. The results of the quantum TDSE and classical calculation in Fig. 4 agree with each other qualitatively well.

We may emphasize that the retrieval of the rescattering momentum via Eq. (7) does not involve any knowledge of the parameters of the MIR field, such as intensity, pulse shape, or carrier envelope phase, some of which are often difficult to be precisely measured in experiment. Thus, rescattering momenta may be obtained in an alternative procedure as compared to the present estimates mainly based on classical calculations which prerequest all information of the probe pulse. This may help to improve the calculation of electron-ion rescattering differential cross sections, and hence methods such as laser-assisted molecular imaging [36–38].

IV. CONCLUSIONS

In conclusion, superelastic rescattering is demonstrated for the prototypical helium atom in strong laser fields. During superelastic rescattering, the free electron extracts the energy stored in He^{+*} by deexciting the second electron to the ground state. The contribution to the photoelectron momentum spectra due to the superelastic rescattering process carries information about the momentum of the returning electron at the instant of rescattering. This may provide improvements to obtain the electron-ion rescattering cross section, since knowledge about the probe laser parameters is not required. We expect that superelastic rescattering occurs in general for other atoms or molecules as well, and offers a new perspective of time-resolved atomic/molecular imaging.

ACKNOWLEDGEMENTS

We thank A. Becker for fruitful discussions. This work was supported by NSF of China (Grant No. 11322438, 11574205). A.J.-B. was supported by the U.S. National Science Foundation under Grant No. 1125844 and by the Air Force Office of Scientific Research (Award No. FA9550-16-1-0121). Simulations were performed on the π supercomputer at Shanghai Jiao Tong University.

- [1] F. Krausz and M. Ivanov, *Attosecond physics*, Rev. Mod. Phys. **81**, 163 (2009).
- [2] P. Agostini and L. F. DiMauro, *The physics of attosecond light pulses*, Rep. Prog. Phys. **67**, 1563 (2004).
- [3] M. F. Kling and M. J. J. Vrakking, *Attosecond electron dynamics*, Annu. Rev. Phys. Chem. **59**, 463 (2008).
- [4] P. B. Corkum and F. Krause, *Attosecond science*, Nature Phys. **3**, 381 (2013).
- [5] F. Lépine, M. Yu. Ivanov and M. J. J. Vrakking, *Attosecond molecular dynamics: fact or fiction?*, Nature Photon. **8**, 195 (2014).
- [6] P. B. Corkum, *Recollision physics*, Phys. Today **64**, 36 (2011)
- [7] W. Becker, X. J. Liu, P. J. Ho and J. H. Eberly, *Theories of photoelectron correlation in laser-driven multiple atomic ionization*, Rev. Mod. Phys. **84**, 1011 (2012)
- [8] M. Uiberacker, Th. Uphues, M. Schultze, A. J. Verhoef, V. Yakovlev, M. F. Kling, J. Rauschenberger, N. M. Kabachnik, H. Schröder, M. Lezius, K. L. Kompa, H.-G. Muller, M. J. J. Vrakking, S. Hendel, U. Kleineberg, U. Heinzmann, M. Drescher and F. Krausz, *Attosecond real-time observation of electron tunnelling in atoms*, Nature **446**, 627 (2007).
- [9] P. B. Corkum, *Plasma perspective on strong field multiphoton ionization*, Phys. Rev. Lett. **71**, 1994 (1993).
- [10] M. Lewenstein, P. Balcou, M. Y. Ivanov, A. LHuillier and P. B. Corkum, *Theory of high-harmonic generation by low-frequency laser fields*, Phys. Rev. A **49**, 2117 (1994).
- [11] G. Sansone, L. Poletto and M. Nisoli, *High-energy attosecond light sources*, Nature Photon. **5**, 655 (2011).
- [12] B. Walker, B. Sheehy, L. F. DiMauro, P. Agostini, K. J. Schafer and K. C. Kulander, *Precision measurement of strong field double ionization of helium*, Phys. Rev. Lett. **73**, 1227 (1994).
- [13] A. Becker and F.H.M. Faisal, *Interpretation of momentum distribution of recoil ions from laser induced non-sequential double ionization*, Phys. Rev. Lett. **84**, 3546 (2000).
- [14] C. Faria and X. Liu, *Electron-electron correlation in strong laser fields*, J. Mod. Opt. **58**, 1076 (2011).
- [15] B. Feuerstein, R. Moshhammer, D. Fischer, A. Dorn, C. D. Schröter, J. Deipenwisch, J.R. Crespo Lopez-Urrutia, C. Höhr, P. Neumayer, J. Ullrich, H. Rottke, C. Trump, M. Wittmann, G. Korn and W. Sandner, *Separation of recollision mechanisms in nonsequential strong field double ionization of Ar: The role of excitation tunneling*, Phys. Rev. Lett. **87**, 043003 (2001).
- [16] Y. Liu, S. Tschuch, A. Rudenko, M. Dürr, M. Siegel, U. Morgner, R. Moshhammer and J. Ullrich, *Strong-field double ionization of Ar below the recollision threshold*, Phys. Rev. Lett. **101**, 053001 (2008).
- [17] Y. Deng, Z. Zeng, Z. Jia, P. Komm, Y. Zheng, X. Ge, R. Li and G. Marcus, *Ultrafast excitation of an inner-shell electron by laser-induced electron recollision*, Phys. Rev. Lett. **116**, 073901 (2016).
- [18] H. Niikura, F. Légaré, R. Hasbani, A. D. Bandrauk, M. Yu. Ivanov, D. M. Villeneuve and P. B. Corkum, *Sub-laser-cycle electron pulses for probing molecular dynamics*, Nature (London) **417**, 917 (2002).
- [19] H. Niikura, F. Légaré, R. Hasbani, M. Yu. Ivanov, D. M. Villeneuve and P. B. Corkum, *Probing molecular dynamics with attosecond resolution using correlated wave packet pairs*, Nature (London) **421**, 826 (2003).
- [20] A. S. Alnaser, T. Osipov, E. P. Benis, A. Wech, B. Shan, C. L. Cocke, X. M. Tong and C. D. Lin, *Rescattering double ionization of D₂ and H₂ by intense laser pulses*, Phys. Rev. Lett. **91**, 163002 (2003).
- [21] M. F. Kling, Ch. Siedschlag, A. J. Verhoef, J. I. Khan, M. Schultze, Th. Uphues, Y. Ni, M. Uiberacker, M. Drescher, F. Krausz and M. J. J. Vrakking, *Control of electron localization in molecular dissociation*, Science **312**, 246 (2006).
- [22] C. I. Blaga, J. Xu, A. D. DiChiara, E. Sistrunk, K. Zhang, P. Agostini, T. A. Miller, L. F. DiMauro and C. D. Lin, *Imaging ultrafast molecular dynamics with laser-induced electron diffraction*, Nature (London) **483**, 194 (2012).
- [23] G. G. Paulus, F. Lindner, H. Walther, A. Baltuška, E. Goulielmakis, M. Lezius and F. Krausz, *Measurement of the phase of few-cycle laser pulses*, Phys. Rev. Lett. **91**, 253004 (2003).
- [24] C. A. Haworth, L. E. Chipperfield, J. S. Robinson, P. L. Knight, J. P. Marangos and J. W. G. Tisch, *Half-cycle cutoffs in harmonic spectra and robust carrier-envelope phase retrieval*, Nature Phys. **3**, 52 (2006).
- [25] S. X. Hu and L. A. Collins, *Attosecond pump probe: Exploring ultrafast electron motion inside an atom*, Phys. Rev. Lett. **96**, 073004 (2006).
- [26] X. Guan, K. Bartschat and B. I. Schneider, *Dynamics of two-photon double ionization of helium in short intense XUV laser pulses*, Phys. Rev. A **77**, 043421 (2008).
- [27] J. Feist, S. Nagele, R. Pazourek, E. Persson, B. I. Schneider, L. A. Collins and J. Burgdörfer, *Probing electron correlation via attosecond XUV pulses in the two-photon double ionization of helium*, Phys. Rev. A **77**, 043420 (2008).
- [28] R. Pazourek, J. Feist, S. Nagele and J. Burgdörfer, *Attosecond streaking of correlated two-electron transitions in helium*, Phys. Rev. Lett. **108**, 163001 (2012).
- [29] W. C. Jiang, L. Y. Peng, W. H. Xiong and Q. Gong, *Comparison study of electron correlation in one-photon and two-photon double ionization of helium*, Phys. Rev. A **88**, 023410 (2013).
- [30] A. Liu and U. Thumm, *Criterion for distinguishing sequential from nonsequential contributions to the double ionization of helium in ultrashort extreme-ultraviolet pulses*, Phys. Rev. Lett. **115**, 183002 (2015).
- [31] M. Lein, E. K. U. Gross and V. Engel, *Intense-field double ionization of helium: identifying the mechanism*, Phys. Rev. Lett. **85**, 4707 (2000).
- [32] J. Zhao and M. Lein, *Probing Fano resonances with ultrashort pulses*, New J. Phys. **14**, 065003 (2012).
- [33] Z. Q. Yang, D. F. Ye, T. Ding, T. Pfeifer and L. B. Fu, *Attosecond XUV absorption spectroscopy of doubly excited states in helium atoms dressed by a time-delayed femtosecond infrared laser*, Phys. Rev. A **91**, 013414 (2015).
- [34] F. He, C. Ruiz and A. Becker, *Absorbing boundaries in numerical solutions of the time-dependent Schrödinger equation on a grid using exterior complex scaling*, Phys. Rev. A **75**, 053407 (2007).
- [35] See the supplemental movie.
- [36] M. Lein, *Molecular imaging using recolliding electrons*, J. Phys. B **40**, R135 (2007).

- [37] T. Morishita, A.-T. Le, Z. Chen and C. D. Lin, *Accurate retrieval of structural information from laser-induced photoelectron and high-order harmonic spectra by few-cycle laser pulses*, Phys. Rev. Lett. **100**, 013903 (2008).
- [38] Y. Zhou, O. I. Tolstikhin and T. Morishita, *Near-forward rescattering photoelectron holography in strong-field ionization: extraction of the phase of the scattering amplitude*, Phys. Rev. Lett. **116**, 173001(2016).